JPET Fast Forward. Published on December 8, 2020 as DOI: 10.1124/jpet.120.000315
This article has not been copyedited and formatted. The final version may differ from this version.

Pharmacology and mechanism of action of HSK16149, a selective ligand of α2δ subunit of voltage-gated calcium channel with analgesic activity in animal models of chronic pain

Xiaoli Gou, Xiaojuan Yu, Dongdong Bai, Bowei Tan, Pingfeng Cao, Meilin Qian, Xiaoxiao Zheng, Lei Chen, Zongjun Shi, Yao Li, Fei Ye, Yong Liang* and Jia Ni*

Haisco Pharmaceutical Group Co., Ltd., 136 Baili Road, Wenjiang district, Chengdu 611130, China.

JPET Fast Forward. Published on December 8, 2020 as DOI: 10.1124/jpet.120.000315
This article has not been copyedited and formatted. The final version may differ from this version.

Running Title:

Pharmacologic profiles of HSK16149

***Corresponding author:** Yong Liang and Jia Ni

Haisco Pharmaceutical Group Co., Ltd.

136 Baili Road, Wenjiang District, Chengdu 611130, China.

Tel: +(86)-028-67250549

Fax: +(86)-028-67250380

E-mail: liangy@haisco.com; nijia@haisco.com

Number of text pages: 49

Number of tables: 4

Number of figures: 9

Number of references: 40

Number of words in Abstract: 250

Number of words in Introduction: 335

Number of words in Discussion: 658

Abbreviations:

AUC: area under the curve

ANOVA: analysis of variance

CCI: chronic constriction injury

JPET Fast Forward. Published on December 8, 2020 as DOI: 10.1124/jpet.120.000315
This article has not been copyedited and formatted. The final version may differ from this version.

CI: confidence interval

C_{max}: maximum concentration

CNS: central nervous system

IC_{50}: 50% inhibitory concentration

ICS: intermittent cold stress

MED: minimum effective dose

PWT: paw withdrawal threshold

SD: standard deviation

STZ: streptozotocin

VGCC: voltage-gated calcium channel

Recommended section:

Drug Discovery and Translational Medicine

JPET Fast Forward. Published on December 8, 2020 as DOI: 10.1124/jpet.120.000315
This article has not been copyedited and formatted. The final version may differ from this version.

Abstract

Chronic pain is a public health problem as current treatments are unsatisfactory with small therapeutic index. Although pregabalin is effective for treating chronic pain, the clinical use is limited due to its side effects. Therefore, improving its therapeutic index is essential. In this study, HSK16149 was found to be a novel ligand of voltage-gated calcium channel (VGCC) $\alpha_2\delta$ subunit. HSK16149 inhibited [^{3}H]gabapentin binding to the $\alpha_2\delta$ subunit and was 23 times more potent than pregabalin. In two rat models of neuropathic pain, the minimum effective dose (MED) of HSK16149 was 10 mg/kg and the efficacy was similar to that of 30 mg/kg pregabalin. Moreover, the efficacy of HSK16149 could persist up to 24 h post-administration at 30 mg/kg, while the efficacy of pregabalin lasted only for 12 h at 30 mg/kg in streptozotocin-induced diabetic neuropathy model, indicating that HSK16149 might be a longer-acting drug candidate. HSK16149 could also inhibit mechanical allodynia in intermittent cold stress model and decrease phase II pain behaviors in formalin-induced nociception model. In addition, the locomotor activity test showed that the MED of HSK16149 was similar to that of pregabalin, while in the rotarod test, the MEDs of HSK16149 and pregabalin were 100 mg/kg and 30 mg/kg, respectively. These finding indicated that HSK16149 might have a better safety profile on the central nervous system. In summary, HSK16149 is a potent ligand of VGCC $\alpha_2\delta$ subunit with a better therapeutic index than pregabalin. Hence, it could be an effective and safe drug candidate for treating chronic pain.

JPET Fast Forward. Published on December 8, 2020 as DOI: 10.1124/jpet.120.000315
This article has not been copyedited and formatted. The final version may differ from this version.

Significance statement:

As a novel potent ligand of VGCC $\alpha_2\delta$ subunit, HSK16149 has the potential to be an effective and safe drug candidate for the treatment of chronic pain.

JPET Fast Forward. Published on December 8, 2020 as DOI: 10.1124/jpet.120.000315
This article has not been copyedited and formatted. The final version may differ from this version.

Introduction

Chronic pain is a long-term debilitating disease that affects normal work and daily life of patients (Tsuda et al., 2011; Vicuna et al., 2015; Tramullas et al., 2018) and is mainly categorized as inflammatory or neuropathic (Liu et al., 2008; Beggs, et al., 2012). However, the exact pathological mechanisms underlying chronic pain remain to be unmasked, which impedes the development of new treatments for chronic pain (Li, et al., 2011; Zhao, et al., 2013). Presently, the common medication management for chronic pain consists of non-steroidal anti-inflammatory drugs, tricyclic antidepressants, serotonin-norepinephrine reuptake inhibitors, and opioids (Cohen et al., 2015). Unfortunately, a subset of patients is refractory to the currently available treatments with limited clinical applicability due to severe side effects (Wang et al., 2011). Moreover, opioids cannot be continually used due to tolerance and physical dependence. Therefore, it is necessary to develop a new treatment for chronic pain.

Gabapentin and pregabalin belonging to gabapentinoids, are selective ligands of voltage-gated calcium channel $\alpha_2\delta$ subunit (Boroujerdi et al., 2011), and were originally used for the treatment of epilepsy (Coderre et al., 2005, Kavoussi, 2006). At a later stage, the antinociceptive effect of these drugs was detected (Sills, 2006). Since approved, gabapentin and pregabalin have extremely improved the life quality of patients suffering from chronic pain, especially neuropathic pain. However, the use of these drugs is usually accompanied by some undesirable side effects, such as dizziness, somnolence, and peripheral edema. Hence, it is advisable to improve this class of drugs, i.e., retain or increase their efficacy and decrease the side effects.

In this study, HSK16149 bound to α2δ subunit with a high affinity *in vitro*. In addition, the *in vivo* assays also proved the potential analgesic effects of HSK16149 in neuropathic pain, fibromyalgia,

JPET Fast Forward. Published on December 8, 2020 as DOI: 10.1124/jpet.120.000315
This article has not been copyedited and formatted. The final version may differ from this version.

and inflammatory pain. Furthermore, HSK16149 showed fewer effects on the central nervous system (CNS) in the rotarod and the locomotor activity tests. Therefore, HSK16149 is a novel and potent ligand for the α2δ subunit of voltage-gated calcium channels (VGCCs) with a better therapeutic index than pregabalin.

JPET Fast Forward. Published on December 8, 2020 as DOI: 10.1124/jpet.120.000315
This article has not been copyedited and formatted. The final version may differ from this version.

Materials and methods

Animals

Male Sprague – Dawley (SD) and Wistar rats weighing 160 – 180 g were purchased from Beijing Vital River Laboratory Animal Technology Co., Ltd. Male C57/BL6 mice weighing 18 – 25 g and male ICR mice weighing 25 – 35 g were obtained from Shanghai SLAC Laboratory Animal Co., Ltd. All animals were maintained on a standard 12 h light/12 h dark cycle with free access to food and water. Those who conducted pain assessment were blinded to the treatment conditions. All experimental procedures were performed in accordance with the guidelines of National Institutes of Health for the handling and use of laboratory animals and the Guidelines of the Institutional Animal Care and Use Committee of Haisco Pharmaceutical Group Co., Ltd (China).

Drugs and reagents

HSK16149 [2-((1S,2S,3R,6S,8S)-2-(aminomethyl)tricyclo[4.2.1.$0^{3,8}$]nonan-2-yl)acetic acid benzenesulfonic acid (1:1)] was synthesized in Haisco Pharmaceutical Group Co., Ltd and the chemical structure of HSK16149 is shown in Figure 1A. Pregabalin was obtained from Hunan Boheng Pharmaceutical Co., Ltd. HSK16149 and pregabalin were solubilized in dimethyl sulfoxide (DMSO) for *in vitro* assays. In animal experiments, the two compounds were suspended in 0.5% carboxymethylcellulose sodium or methylcellulose and orally administered at a volume of 10 μL/g. Streptozotocin (STZ) was purchased from Chengdu Dingdang Pharmaceutical Co., Ltd. All reagents were of analytical grade unless otherwise stated.

[^{3}H]gabapentin binding assay

Male Wistar rats were killed by decapitation and craniotomy was conducted for each animal. The whole brain was collected, the meninges were peeled off, and the cortex was removed with

JPET Fast Forward. Published on December 8, 2020 as DOI: 10.1124/jpet.120.000315
This article has not been copyedited and formatted. The final version may differ from this version.

forceps and tweezers. Fresh cerebral cortical membranes were homogenized in modified 10 mM HEPES buffer (pH 7.4) with Bertin Precellys Evolution. The pellet was collected by centrifugation of the homogenate at 12000 $\times g$ for 20 min at 4 °C. An equivalent of 0.02 mg of the membrane was incubated with 20 nM [^{3}H]gabapentin in the presence of varying concentrations of test compounds for 30 min at 25 °C. Bound and free fractions were separated by vacuum filtration through a GF/B filter pretreated with 0.3% polyetherimide. Then, the filters were washed with ice-cold buffer. Bound radioactivity was determined using liquid scintillation counting (Suman-Chauhan et al., 1993; Gee et al., 1996). Non-specific binding was defined in the presence of 100 μM gabapentin (Vincent et al., 2016). The percentage inhibition of [^{3}H]gabapentin binding was calculated as follows: inhibition rate (%) = (CPM_{total}-$CPM_{compound}$) / (CPM_{total}-$CPM_{non\text{-}specific}$), where CPM_{total} = total [^{3}H]gabapentin bound (membrane + 20 nM [^{3}H]gabapentin) and $CPM_{non\text{-}specific}$ = non-specific [^{3}H]gabapentin bound (membrane + 20 nM [^{3}H]gabapentin + 100 μM gabapentin). The 50% inhibitory concentration (IC_{50}) was determined by non-linear, least squares regression analysis using GraphPad Prism 8.3.0 (San Diego, CA, USA).

***In vitro* off-target pharmacological profile**

The *in vitro* pharmacological activities of HSK16149 on 105 receptors, ion channels, transporters and enzymes were evaluated based on radioligand binding and enzyme assays at Eurofins Panlabs Discovery Services Taiwan, Ltd. The assay services included SafetyScreen87 Panel (Item PP223) and 18 additional radioligand binding and enzyme assays (Domon et al., 2018).

Chronic constriction injury model

The chronic constriction injury (CCI) model of neuropathic pain was established on the left side. Briefly, under inhaled isoflurane anesthesia, the femoral skin was incised and the sciatic nerve was

JPET Fast Forward. Published on December 8, 2020 as DOI: 10.1124/jpet.120.000315
This article has not been copyedited and formatted. The final version may differ from this version.

exposed with a pair of forceps (Ghoreishi-Haack et al., 2018). A 2-mm-long polyethylene cuff was successively implanted around the nerve (Bailey and Ribeiro-da-Silva, 2006; Balasubramanyan et al., 2006). Then, the incision was closed with a skin stapler and the rats were returned to their cages after recovering from anesthesia. The pharmacological effects of mirogabalin were evaluated on day 17 post-CCI. On the test day, the 50% paw withdraw threshold (50% PWT) was determined using Dixon's up-down method before dosing (baseline value). The animals were grouped according to the baseline value and orally administered 0.5% carboxymethylcellulose sodium solution or mirogabalin at a volume of 10 μL/g. Subsequently, PWTs were measured at 2, 4 and 6 h post-dosing. The area under the curve (AUC, 50% PWT *vs.* time) was calculated using the trapezoid rule. The satellite groups were set (N=4), and plasma was collected at the following time points: 0, 0.083, 0.25, 0.5, 1, 2, 6, 12, and 24 h post-dosing. The plasma concentrations of HSK16149 and pregabalin were detected using a validated liquid chromatography–tandem mass spectrometry method.

STZ-induced diabetic neuropathy

Male SD rats were acclimated to the laboratory for 5 – 7 days before study initiation, and the mechanical pain thresholds of rats were detected three times. Rats whose 50% PWT was not smaller than 15 g, were intraperitoneally administered 70 mg/kg of STZ in 0.1 mol/L citrate buffer (pH 4.4) for three successive days. A total of 22 days after the first STZ injection, the levels of blood glucose were measured using a glucose meter, and the animals with fasted glucose levels >11.1 mmol/L were defined as diabetic rats. Subsequently, the pain thresholds of diabetic rats were measured and defined as baseline PWT values (pre-dose). The animals were randomized based on the baseline and orally administered 0.5% carboxymethylcellulose sodium solution

JPET Fast Forward. Published on December 8, 2020 as DOI: 10.1124/jpet.120.000315
This article has not been copyedited and formatted. The final version may differ from this version.

(vehicle control group) or test compounds (treatment groups) at a volume of 10 μL/g. Then, the PWTs were measured at different time points. The AUC (50% PWT *vs.* time) was calculated by a trapezoid rule. The satellite groups were set (N=4), and the plasma was collected at the following time points: 0, 0.083, 0.25, 0.5, 1, 2, 6, 12, and 24 h post-dosing. The plasma concentrations of HSK16149 and pregabalin were detected with a validated liquid chromatography–tandem mass spectrometry method.

Intermittent cold stress model

C57/BL6 mice were exposed to intermittent cold stress (ICS), as previously reported (Nishiyori and Ueda, 2008; Mukae et al., 2016). Firstly, the mice were kept in stainless cages at an overnight temperature of 4 °C from 16:30 on day 0 to 10:00 on day 1, following which, the animals were placed in an environment with room temperature (24 ± 2 °C) and returned to the cold environment (4 °C) after 30 min. The mice were then transferred between the room temperature and the cold environment every 30 min until 16:30 on day 1. The above procedures were repeated once from day 1 to day 2. Subsequently, the mice were kept again in the cold environment from 16:30 on day 2 to 10:00 on day 3 (Saeki et al., 2019). Finally, the mice were returned and adapted to the room temperature. The pain test (baseline value) was implemented on day 4 and mice with 50% PWT over 0.5 g were excluded. Finally, the animals were divided into different groups according to the baseline value and orally administered 0.5% methylcellulose solution or test compounds. The mechanical pain thresholds were detected at 2 h post-drug administration.

Mechanical pain threshold test

Paw withdrawal responses to mechanical stimuli were measured using a set of von Frey filaments (Stoelting, US). Before each testing cycle, each animal was habituated to a Plexiglas chamber on a

JPET Fast Forward. Published on December 8, 2020 as DOI: 10.1124/jpet.120.000315
This article has not been copyedited and formatted. The final version may differ from this version.

metallic mesh floor for a 30-min to 1-h period (Kawasaki et al., 2008; Sakai et al., 2013; Gazzo et al., 2019). For mice, a series of calibrated von Frey filaments in log increments of force (0.02 – 1.4 g) was applied to the plantar surface of the affected paws below the mesh floor. The paw withdrawal responses of rats were determined in the same manner but using von Frey filaments over a range of 1 – 15 g (Lai et al., 2006; Xie et al., 2017; Zhao et al., 2017). The 50% PWT was determined using Dixon's up-down method (Chaplan et al., 1994; Weir et al., 2017).

Formalin-induced nociception

After administration of the test compounds or vehicle (0.5% methylcellulose solution), ICR mice were subcutaneously injected with 15 μL of 2.5% formalin solution into the back of the right hind paw and placed into an automatic detector (Ponsati et al., 2012). Licking or biting of the injected paw (motion counts) was recorded as a nociceptive response, and the mice were observed from 0 – 9 min (neurogenic phase, phase I) and 10 – 45 min (inflammatory phase, phase II) post-formalin injection (Brittain et al., 2011; Shin et al., 2012).

Rotarod test

An accelerating rotarod apparatus was used to measure the impact of the test compounds on motor coordination (Shiotsuki et al., 2010; Sakai et al., 2017; Slivicki et al., 2018). Rats were placed on a 6-cm-diameter rod that was accelerated to 15 rpm. The duration of staying on the rod was recorded for all the rats. Each rat was evaluated three times, and the average value was defined as the fall-off latency. Rats were trained for three successive days, and those with fall-off latency of >90 s (baseline value) on day 3 were moved on to the test session. On day 4, the rats were grouped according to the baseline value and orally administered 0.5% methylcellulose solution or test compounds. At 2 h after dosing, the fall-off latency for each rat was recorded again. The

JPET Fast Forward. Published on December 8, 2020 as DOI: 10.1124/jpet.120.000315
This article has not been copyedited and formatted. The final version may differ from this version.

maximum fall-off latency was set at 120 s.

Locomotor activity test

The locomotor activity was tracked and analyzed using an ANY-maze video tracking system. After acclimatizing to the chamber for two days, the rats were administered either vehicle or test compounds and placed into the detection system at 2 h post-dosing. Each rat was then allowed to explore the field for 1 h and the total distance traveled was analyzed (Kraeuter et al., 2019).

Statistical analysis

All data were expressed as mean ± SD and none was excluded. Shapiro-Wilk test was employed to assess whether the data followed a normal distribution. All data were analyzed by two-tailed, unpaired t-test, unpaired Mann-Whitney U test, one-way analysis of variance (ANOVA) with Dunnett's comparisons, Kruskal-Wallis test with Dunn's comparisons, or two-way ANOVA with Dunnett's comparisons. All statistical tests were performed using GraphPad Prism 8.3.0 (San Diego, CA, USA). $P<0.05$ indicated statistical significance.

JPET Fast Forward. Published on December 8, 2020 as DOI: 10.1124/jpet.120.000315
This article has not been copyedited and formatted. The final version may differ from this version.

Results

Binding affinity to VGCC $\alpha_2\delta$ subunit

The binding affinity of the compound to VGCC $\alpha_2\delta$ subunit was assayed by a competitive [^{3}H]gabapentin binding assay. As shown in Figure 1B, both HSK16149 and pregabalin could prevent [^{3}H]gabapentin from binding in a dose-dependent manner. The IC_{50} of HSK16149 and pregabalin were 3.96 nM (95% CI: 2.28 – 6.63 nM) and 92.12 nM (95% CI: 61.40 – 141.2 nM), respectively. Therefore, HSK16149 is a potent ligand of VGCC $\alpha_2\delta$ subunit, which exhibited stronger pharmacological activity than pregabalin.

In vitro off-target pharmacological profile

In order to assess the in vitro target selectivity of HSK16149, its pharmacological activities on 105 targets were evaluated and an inhibition or stimulation rate of > 50% was considered as a significant response. Surprisingly, HSK16149 had no significant effects on any of the targets at the concentration of 10 μM (Supplemental Table 1). Therefore, it can be concluded that HSK16149 is selective ligand for the α2δ subunit of VGCCs.

Analgesic effects in CCI-induced neuropathic pain model

As one of the most commonly used neuropathic pain models, the CCI model was employed to evaluate the analgesic effects of HSK16149 and pregabalin. Seventeen days after the surgery, HSK16149 and pregabalin were orally administered, and the effects on the mechanical pain threshold were determined after dosing. The data showed that both HSK16149 and pregabalin could increase the PWT in a dose-dependent manner (Figure 2). In the 30 mg/kg HSK16149 group, the 50% PWT value was 3.24-fold larger than that in the vehicle-treated group (P<0.001) at 2 h, and peaked at 6 h after dosing (Figure 2A). The effects of 10 mg/kg HSK16149 on mechanical

JPET Fast Forward. Published on December 8, 2020 as DOI: 10.1124/jpet.120.000315
This article has not been copyedited and formatted. The final version may differ from this version.

pain thresholds were similar to the 30 mg/kg HSK16149-treated group at 2 h (12.93 g *vs.* 11.93 g) or 4 h (13.66 g *vs.* 13.55 g). Although the 50% PWT value in 10 mg/kg HSK16149-treated group was lower than that in the 30 mg/kg HSK16149-treated group (P=0.004, t-test) at 6 h, the effect of 10 mg/kg HSK16149 was similar to the 30 mg/kg pregabalin-treated group (P=0.29, Mann-Whitney test). In addition, compared to the vehicle-treated group, 3 mg/kg of HSK16149 induced a significant increase of 50% PWT value at 4 h (7.33 g *vs.* 3.11 g, P=0.008). Typically, the pharmacological activities were comparable to each other in 10 or 30 mg/kg HSK16149 or 30 mg/kg pregabalin-treated groups (Figure 2D). On the other hand, the effect of 10 mg/kg pregabalin was lower than that of 30 mg/kg pregabalin (43.90 *vs.* 64.82, P=0.0012; Figure 2E). When administered at the maximal dose (30 mg/kg), HSK16149 and pregabalin exhibited significant effects on the 50% PWT values with a 2-fold increase at 8 h post-dosing. In order to calculate the therapeutic index, the minimum effective dose (MED) was obtained by defining the lowest dose that markedly increased the AUC (50% PWT *vs.* time). The MED was 10 mg/kg for both HSK16149 and pregbalin. Considering the weaker activity of 10 mg/kg pregabalin (*vs.* 30 mg/kg pregabalin) and the comparability of the AUC value between 10 mg/kg HSK16149 and 30 mg/kg pregabalin, we speculated that HSK16149 might provide better improvement for patients suffering from neuropathic pain.

The pharmacokinetic parameters of HSK16149 and pregabalin are shown in Table 1. The exposure levels (C_{max} and $AUC_{0\text{-}24h}$) in the plasma increased in a dose-proportional manner, and the $AUC_{0\text{-}24h}$ of HSK16149 was 2.25 – 4.73 times lower than that of pregabalin.

Analgesic effects in STZ-induced diabetic neuropathy model

The analgesic effects produced by HSK16149 and pregabalin were tested in STZ-induced diabetic

JPET Fast Forward. Published on December 8, 2020 as DOI: 10.1124/jpet.120.000315
This article has not been copyedited and formatted. The final version may differ from this version.

neuropathy model. On the day of testing, different doses of HSK16149 and pregabalin were orally administered to SD rats. As shown in Figure 3, both HSK16149 and pregabalin increased the PWT in a dose-dependent manner. Compared to the vehicle group, HSK16149 at 30 mg/kg obviously increased the 50% PWT value at 2 h post-dosing (10.35 g *vs.* 3.91 g, P=0.021), and the efficacy could persist up to 6 h post-dosing with a slight increase. Although no statistical significance was detected, the 50% PWT value in the 10 mg/kg HSK16149 group was 2.4 times larger than that of the vehicle group at 2 h post-dosing (P=0.051), and HSK16149 at 10 mg/kg could significantly increase the 50% PWT value at 4 h (10.55 g *vs.* 4.35 g, P=0.016) or 6 h (11.74 g *vs.* 4.24 g, P=0.0026) after dosing. In the 3 mg/kg HSK16149 group, the PWT value was approximately doubled at 6 h post-dose (*vs.* vehicle group; Figure 3A). The MED was defined as the lowest dose level that statistically increased the AUC (50% PWT *vs.* time). The MED of HSK16149 was 10 mg/kg (P=0.016 *vs.* vehicle) and no statistically significant difference was detected in the efficacy between 10 mg/kg and 30 mg/kg, which was comparable to that of pregabalin at 30 mg/kg (Figure 3D). On the other hand, the MED of pregabalin was also determined to be 10 mg/kg (P=0.0035 *vs.* vehicle). However, the efficacy of 10 mg/kg pregabalin was remarkably inferior to 30 mg/kg pregabalin (P=0.0008, Figure 3B and 3E). In addition, the efficacy of a single-dose HSK16149 could persist up to 8 h at 10 mg/kg and 24 h at 30 mg/kg. In comparison, the analgesic effect of pregabalin was lost at 8 h for 10 mg/kg, and at 24 h for 30 mg/kg after drug administration (Figure 3C). The data showed that HSK16149 might have a strong potency, which was longer-acting than pregabalin.

The pharmacokinetic parameters of HSK16149 and pregabalin are shown in Table 1. The data are similar to those in the CCI-induced neuropathic pain model. The exposure levels (C_{max} and

JPET Fast Forward. Published on December 8, 2020 as DOI: 10.1124/jpet.120.000315
This article has not been copyedited and formatted. The final version may differ from this version.

$AUC_{0\text{-}24h}$) in plasma increased in a dose-dependent manner, and the $AUC_{0\text{-}24h}$ of HSK16149 was 2.67 – 4.33 times lower than that of pregabalin.

Antinociceptive effects in a mouse model of fibromyalgia

The antinociceptive effects of HSK16149 and pregabalin in fibromyalgia were evaluated using an ICS model, which is one of well-established mouse models of fibromyalgia. On the day of the test, different doses of HSK16149 and 30 mg/kg pregabalin were orally administered to the mice at 2 h pre-testing. As shown in Figure 4A, intermittent cold stress exposure dramatically induced hypersensitivity to mechanical stimulation in mice with an obvious decrease in 50% PWT (from 1.22 g to 0.32 g). Furthermore, HSK16149 inhibited mechanical allodynia in a dose-dependent manner. The MED of HSK16149 was 30 mg/kg in this assay (P=0.0005 *vs.* vehicle). Compared to the vehicle group, HSK16149 at 30 mg/kg induced a 2.6-fold increase in 50% PWT and the efficacy was comparable to 30 mg/kg pregabalin (Figure 4B).

Effects on pain behaviors in an inflammatory pain model

A formalin-induced pain model was used to assess the pharmacological effects of HSK16149 and pregabalin. In this model, different doses of HSK16149 and 30 mg/kg pregabalin were administered at 2 h pre-testing, following formalin injection into the mice's hind paws, causing a two-phase pattern of behavior responses (phase I and phase II). Consequently, we observed that HSK16149 decreased formalin-induced pain behaviors in phase II in a dose-dependent manner. Both 10 mg/kg and 30 mg/kg HSK16149 significantly decreased formalin-induced pain behaviors in phase II with a 1.6- and 2.2-fold decrease in motion counts, respectively (P<0.0001 *vs.* vehicle). The effect of 30 mg/kg HSK16149 was similar to that of pregabalin at the same dose (P=0.56, Figure 5B). Both HSK16149 and pregabalin had slight effects on formalin-induced pain behaviors

JPET Fast Forward. Published on December 8, 2020 as DOI: 10.1124/jpet.120.000315
This article has not been copyedited and formatted. The final version may differ from this version.

in phase I at a dose of 30 mg/kg, although not significantly (Figure 5A).

Effects on central nervous system

Reportedly, VGCC inhibition is related to the side effects on CNS, such as ataxia and sedation. A rotarod test was used to test the ataxic effects of HSK16149 and pregabalin. In this assay, different doses of HSK16149 and pregabalin were orally administered to SD rats at 2 h before the test. At a dose of 100 mg/kg, both HSK16149 and pregabalin produced ataxic side effects with a 1.8- and 3.6-fold decrease in the fall-off latency, respectively, and HSK16149 had a milder effect on ataxia than pregabalin (P=0.012). Notably, pregabalin at 30 mg/kg attenuated the ability of rats to maintain their position on an accelerating rotarod (P=0.043 *vs.* vehicle, a 1.4-fold decrease). However, HSK16149 at 30 mg/kg did not show any ataxic effect (P=0.28 *vs.* vehicle, Figure 6A).

The sedative effects of HSK16149 and pregabalin at 2 h post-dosing were evaluated by a locomotor activity test. As shown in Figure 6B, both HSK16149 and pregabalin reduced the total distance traveled by the rats within 1 h in the chambers in a dose-dependent manner. The MED was 100 mg/kg for both HSK16149 and pregabalin (P<0.0001 *vs.* vehicle, a 3-fold decrease), and the effect of HSK16149 on sedation was the same as that of pregabalin at the same dose.

JPET Fast Forward. Published on December 8, 2020 as DOI: 10.1124/jpet.120.000315
This article has not been copyedited and formatted. The final version may differ from this version.

Discussion

Pregabalin was approved for treating neuropathic pain in 2004 and has significantly improved the life quality of patients who suffered from chronic pain. However, undesirable side effects, such as dizziness, somnolence, and peripheral edema, are exposed in treatment (Calandre et al., 2016). Therefore, developing new treatments for chronic pain with improved efficacy and fewer side effects is a great challenge. This study aimed to find a novel potent VGCC $\alpha_2\delta$ subunit ligand with better efficacy and safety profiles.

The *in vitro* binding studies showed that both HSK16149 and pregabalin showed a high affinity to the $\alpha_2\delta$ subunit of VGCCs. HSK16149 was more potent (23-fold) than pregabalin. In addition, HSK16149 showed no activities on 105 other targets, indicating a good safety profile.

Notably, the *in vitro* pharmacological activities are not completely in accordance with the *in vivo* pharmacological effects in many cases, and binding to the $\alpha_2\delta$ subunit of VGCC might not correlate with *in vivo* analgesic efficacy (Lynch et al., 2006). Therefore, the pharmacological effects of HSK16149 were evaluated in four animal models, including CCI-induced neuropathic pain, STZ-induced diabetic neuropathy, ICS-induced FM-like pain, and formalin-induced nociception. In all these models, HSK16149 exhibited analgesic efficacy in a dose-dependent manner, and the pharmacological activity of HSK16149 was similar to or slightly more potent than that of pregabalin at the same dose. On the other hand, the exposure level of HSK16149 in plasma was markedly lower than that of pregabalin at the same dose. When administered at 30 mg/kg, the exposure level of HSK16149 ($AUC_{0\text{-}6h}$) in the brain tissue was 18-fold lower than that of pregabalin (Supplemental Table 2). These findings indicated that HSK16149 might have fewer side effects at a dose at which the pharmacological activities between HSK16149 and pregabalin

JPET Fast Forward. Published on December 8, 2020 as DOI: 10.1124/jpet.120.000315
This article has not been copyedited and formatted. The final version may differ from this version.

are equipotent.

As previously reported, the major side effects of pregabalin were its effects on CNS. Therefore, the rotarod test and locomotor activity test were performed. The results showed that the ataxic side effects of HSK16149 were weaker than those of pregabalin, and the sedative side effects of HSK16149 were similar to that of pregabalin. The *in vivo* pharmacological and side effect profiles of HSK16149 and pregabalin are summarized in Table 2. The therapeutic indexes were obtained by calculating the ratio of the MEDs producing side effects in the rotarod test or locomotor activity test and the MED in the neuropathic pain model. Strikingly, the safety profiles of HSK16149 were better than those of pregabalin.

Recently, mirogabalin was approved in Japan as another ligand of VGCC $\alpha_2\delta$ subunit. The efficacy and safety profile of mirogabalin was also tested in our laboratory. The IC_{50} of mirogabalin was 6.24 nM (95% CI: 4.47 – 8.64 nM) to inhibit [^{3}H]gabapentin binding to VGCC $\alpha_2\delta$ subunit (Supplemental Figure 1), which was comparable to that of HSK16149. The *in vivo* efficacy of mirogabalin was evaluated in CCI hyperalgesia model in rats. The MED of mirogabalin was 10 mg/kg in this model (Supplemental Figure 2). The effects of mirogabalin on CNS were also tested in the rotarod and locomotor activity tests. The MEDs of mirogabalin were 10 mg/kg and 25 mg/kg, respectively (Supplemental Figure 3). The therapeutic indexes were obtained by calculating the ratio of the MEDs producing side effects in the rotarod test or the locomotor activity test and the MED in the CCI model, thereby indicating that the therapeutic index of HSK16149 is larger than that of mirogabalin (10-fold or 4-fold, Table 2).

Although it is usual that some candidates with good preclinical data show little or no benefits for patients in clinical trials, we await the results from phase II clinical trials of HSK16149. The

JPET Fast Forward. Published on December 8, 2020 as DOI: 10.1124/jpet.120.000315
This article has not been copyedited and formatted. The final version may differ from this version.

subsequent data might prove that HSK16149 is a more potent and safer analgesic drug.

In conclusion, HSK16149 showed promising efficacy in different *in vitro* assays and *in vivo* pain models with fewer CNS side effects. Currently, HSK16149 is under phase II/III clinical trial in China (CTR20202015, https://www.wuxuwang.com/linchuang/49a9d19a-0c7c-11eb-a061-00163e0eafb3). The data strongly support continued clinical trials in various chronic pain conditions.

JPET Fast Forward. Published on December 8, 2020 as DOI: 10.1124/jpet.120.000315
This article has not been copyedited and formatted. The final version may differ from this version.

Acknowledgments

The authors thank Eurofins Panlabs Discovery Services Taiwan Ltd, and Wuxi Apptec Co., Ltd, for their assistance with the experiments.

Declarations of interest

None

Authorship Contributions

Participated in research design: Gou, Ye, Liang, and Ni

Conducted experiments: Gou, Yu, Bai, Tan, Cao, Qian, and Zheng

Contributed new reagents or analytic tools: Chen, Shi, and Li

Performed data analysis: Gou, Ye, and Ni

Wrote or contributed to the writing of the manuscript: Gou, Li, Ye, and Ni

Funding

This work received no external funding.

JPET Fast Forward. Published on December 8, 2020 as DOI: 10.1124/jpet.120.000315
This article has not been copyedited and formatted. The final version may differ from this version.

References

Bailey, A. L. and A. Ribeiro-da-Silva (2006). Transient loss of terminals from non-peptidergic nociceptive fibers in the substantia gelatinosa of spinal cord following chronic constriction injury of the sciatic nerve. Neuroscience 138(2): 675-690.

Balasubramanyan, S., P. L. Stemkowski, M. J. Stebbing and P. A. Smith (2006). Sciatic chronic constriction injury produces cell-type-specific changes in the electrophysiological properties of rat substantia gelatinosa neurons. J Neurophysiol 96(2): 579-590.

Beggs, S., T. Trang and M. W. Salter (2012). P2X4R+ microglia drive neuropathic pain. Nat Neurosci 15(8): 1068-1073.

Boroujerdi, A., J. Zeng, K. Sharp, D. Kim, O. Steward and Z. D. Luo (2011). Calcium channel alpha-2-delta-1 protein upregulation in dorsal spinal cord mediates spinal cord injury-induced neuropathic pain states. Pain 152(3): 649-655.

Brittain, J. M., D. B. Duarte, S. M. Wilson, W. Zhu, C. Ballard, P. L. Johnson, N. Liu, W. Xiong, M. S. Ripsch, Y. Wang, J. C. Fehrenbacher, S. D. Fitz, M. Khanna, C. K. Park, B. S. Schmutzler, B. M. Cheon, M. R. Due, T. Brustovetsky, N. M. Ashpole, A. Hudmon, S. O. Meroueh, C. M. Hingtgen, N. Brustovetsky, R. R. Ji, J. H. Hurley, X. Jin, A. Shekhar, X. M. Xu, G. S. Oxford, M. R. Vasko, F. A. White and R. Khanna (2011). Suppression of inflammatory and neuropathic pain by uncoupling CRMP-2 from the presynaptic Ca(2)(+) channel complex. Nat Med 17(7): 822-829.

Calandre, E. P., F. Rico-Villademoros and M. Slim (2016). Alpha2delta ligands, gabapentin, pregabalin and mirogabalin: a review of their clinical pharmacology and therapeutic use. Expert Rev Neurother 16(11): 1263-1277.

Chaplan, S. R., F. W. Bach, J. W. Pogrel, J. M. Chung and T. L. Yaksh (1994). Quantitative assessment of tactile allodynia in the rat paw. J Neurosci Methods 53(1): 55-63.

Coderre, T. J., N. Kumar, C. D. Lefebvre and J. S. Yu (2005). Evidence that gabapentin reduces neuropathic pain by inhibiting the spinal release of glutamate. J Neurochem 94(4): 1131-1139.

Cohen, K., N. Shinkazh, J. Frank, I. Israel and C. Fellner (2015). Pharmacological treatment of diabetic peripheral neuropathy. P T 40(6): 372-388.

Domon, Y., N. Arakawa, T. Inoue, F. Matsuda, M. Takahashi, N. Yamamura, K. Kai and Y. Kitano (2018). Binding Characteristics and Analgesic Effects of Mirogabalin, a Novel Ligand for the alpha2delta Subunit of Voltage-Gated Calcium Channels. J Pharmacol Exp Ther 365(3): 573-582.

Gazzo, G., P. Girard, N. Kamoun, M. Verleye and P. Poisbeau (2019). Analgesic and anti-edemic properties of etifoxine in models of inflammatory sensitization. Eur J Pharmacol 843: 316-322.

Gee, N. S., J. P. Brown, V. U. Dissanayake, J. Offord, R. Thurlow and G. N. Woodruff (1996). The novel anticonvulsant drug, gabapentin (Neurontin), binds to the alpha2delta subunit of a calcium channel. J Biol Chem 271(10): 5768-5776.

Ghoreishi-Haack, N., J. M. Priebe, J. D. Aguado, E. M. Colechio, J. S. Burgdorf, M. S. Bowers, C. N. Cearley, M. A. Khan and J. R. Moskal (2018). NYX-2925 Is a Novel N-Methyl-d-Aspartate Receptor Modulator that Induces Rapid and Long-Lasting Analgesia in Rat Models of Neuropathic Pain. J Pharmacol Exp Ther 366(3): 485-497.

Kavoussi, R. (2006). Pregabalin: From molecule to medicine. Eur Neuropsychopharmacol 16

Suppl 2: S128-133.

Kawasaki, Y., Z. Z. Xu, X. Wang, J. Y. Park, Z. Y. Zhuang, P. H. Tan, Y. J. Gao, K. Roy, G. Corfas, E. H. Lo and R. R. Ji (2008). Distinct roles of matrix metalloproteases in the early- and late-phase development of neuropathic pain. Nat Med 14(3): 331-336.

Kraeuter, A. K., P. C. Guest and Z. Sarnyai (2019). The Open Field Test for Measuring Locomotor Activity and Anxiety-Like Behavior. Methods Mol Biol 1916: 99-103.

Lai, J., M. C. Luo, Q. Chen, S. Ma, L. R. Gardell, M. H. Ossipov and F. Porreca (2006). Dynorphin A activates bradykinin receptors to maintain neuropathic pain. Nat Neurosci 9(12): 1534-1540.

Li, K. C., F. Wang, Y. Q. Zhong, Y. J. Lu, Q. Wang, F. X. Zhang, H. S. Xiao, L. Bao and X. Zhang (2011). Reduction of follistatin-like 1 in primary afferent neurons contributes to neuropathic pain hypersensitivity. Cell Res 21(4): 697-699.

Liu, X. J., J. R. Gingrich, M. Vargas-Caballero, Y. N. Dong, A. Sengar, S. Beggs, S. H. Wang, H. K. Ding, P. W. Frankland and M. W. Salter (2008). Treatment of inflammatory and neuropathic pain by uncoupling Src from the NMDA receptor complex. Nat Med 14(12): 1325-1332.

Lynch, J. J., 3rd, P. Honore, D. J. Anderson, W. H. Bunnelle, K. H. Mortell, C. Zhong, C. L. Wade, C. Z. Zhu, H. Xu, K. C. Marsh, C. H. Lee, M. F. Jarvis and M. Gopalakrishnan (2006). (L)-Phenylglycine, but not necessarily other alpha2delta subunit voltage-gated calcium channel ligands, attenuates neuropathic pain in rats. Pain 125(1-2): 136-142.

Mukae, T., W. Fujita and H. Ueda (2016). P-glycoprotein inhibitors improve effective dose and time of pregabalin to inhibit intermittent cold stress-induced central pain. J Pharmacol Sci

131(1): 64-67.

Nishiyori, M. and H. Ueda (2008). Prolonged gabapentin analgesia in an experimental mouse model of fibromyalgia. Mol Pain 4: 52.

Ponsati, B., C. Carreno, V. Curto-Reyes, B. Valenzuela, M. J. Duart, W. Van den Nest, O. Cauli, B. Beltran, J. Fernandez, F. Borsini, A. Caprioli, S. Di Serio, M. Veretchy, A. Baamonde, L. Menendez, F. Barros, P. de la Pena, R. Borges, V. Felipo, R. Planells-Cases and A. Ferrer-Montiel (2012). An inhibitor of neuronal exocytosis (DD04107) displays long-lasting in vivo activity against chronic inflammatory and neuropathic pain. J Pharmacol Exp Ther 341(3): 634-645.

Saeki, K., S. I. Yasuda, M. Kato, M. Kano, Y. Domon, N. Arakawa and Y. Kitano (2019). Analgesic effects of mirogabalin, a novel ligand for alpha2delta subunit of voltage-gated calcium channels, in experimental animal models of fibromyalgia. Naunyn Schmiedebergs Arch Pharmacol 392(6): 723-728.

Sakai, A., F. Saitow, M. Maruyama, N. Miyake, K. Miyake, T. Shimada, T. Okada and H. Suzuki (2017). MicroRNA cluster miR-17-92 regulates multiple functionally related voltage-gated potassium channels in chronic neuropathic pain. Nat Commun 8: 16079.

Sakai, A., F. Saitow, N. Miyake, K. Miyake, T. Shimada and H. Suzuki (2013). miR-7a alleviates the maintenance of neuropathic pain through regulation of neuronal excitability. Brain 136(Pt 9): 2738-2750.

Shin, N., M. Covington, D. Bian, J. Zhuo, K. Bowman, Y. Li, M. Soloviev, D. Q. Qian, P. Feldman, L. Leffet, X. He, K. He Wang, K. Krug, D. Bell, P. Czerniak, Z. Hu, H. Zhao, J. Zhang, S. Yeleswaram, W. Yao, R. Newton and P. Scherle (2012). INCB38579, a novel and potent

histamine H(4) receptor small molecule antagonist with anti-inflammatory pain and anti-pruritic functions. Eur J Pharmacol 675(1-3): 47-56.

Shiotsuki, H., K. Yoshimi, Y. Shimo, M. Funayama, Y. Takamatsu, K. Ikeda, R. Takahashi, S. Kitazawa and N. Hattori (2010). A rotarod test for evaluation of motor skill learning. J Neurosci Methods 189(2): 180-185.

Sills, G. J. (2006). The mechanisms of action of gabapentin and pregabalin. Curr Opin Pharmacol 6(1): 108-113.

Slivicki, R. A., Z. Xu, P. M. Kulkarni, R. G. Pertwee, K. Mackie, G. A. Thakur and A. G. Hohmann (2018). Positive Allosteric Modulation of Cannabinoid Receptor Type 1 Suppresses Pathological Pain Without Producing Tolerance or Dependence. Biol Psychiatry 84(10): 722-733.

Suman-Chauhan, N., L. Webdale, D. R. Hill and G. N. Woodruff (1993). Characterisation of [3H]gabapentin binding to a novel site in rat brain: homogenate binding studies. Eur J Pharmacol 244(3): 293-301.

Tramullas, M., R. Frances, R. de la Fuente, S. Velategui, M. Carcelen, R. Garcia, J. Llorca and M. A. Hurle (2018). MicroRNA-30c-5p modulates neuropathic pain in rodents. Sci Transl Med 10(453).

Tsuda, M., Y. Kohro, T. Yano, T. Tsujikawa, J. Kitano, H. Tozaki-Saitoh, S. Koyanagi, S. Ohdo, R. R. Ji, M. W. Salter and K. Inoue (2011). JAK-STAT3 pathway regulates spinal astrocyte proliferation and neuropathic pain maintenance in rats. Brain 134(Pt 4): 1127-1139.

Vicuna, L., D. E. Strochlic, A. Latremoliere, K. K. Bali, M. Simonetti, D. Husainie, S. Prokosch, P. Riva, R. S. Griffin, C. Njoo, S. Gehrig, M. A. Mall, B. Arnold, M. Devor, C. J. Woolf, S. D.

Liberles, M. Costigan and R. Kuner (2015). The serine protease inhibitor SerpinA3N attenuates neuropathic pain by inhibiting T cell-derived leukocyte elastase. Nat Med 21(5): 518-523.

Vincent, K., V. M. Cornea, Y. I. Jong, A. Laferriere, N. Kumar, A. Mickeviciute, J. S. T. Fung, P. Bandegi, A. Ribeiro-da-Silva, K. L. O'Malley and T. J. Coderre (2016). Intracellular mGluR5 plays a critical role in neuropathic pain. Nat Commun 7: 10604.

Wang, H., H. Xu, L. J. Wu, S. S. Kim, T. Chen, K. Koga, G. Descalzi, B. Gong, K. I. Vadakkan, X. Zhang, B. K. Kaang and M. Zhuo (2011). Identification of an adenylyl cyclase inhibitor for treating neuropathic and inflammatory pain. Sci Transl Med 3(65): 65ra63.

Weir, G. A., S. J. Middleton, A. J. Clark, T. Daniel, N. Khovanov, S. B. McMahon and D. L. Bennett (2017). Using an engineered glutamate-gated chloride channel to silence sensory neurons and treat neuropathic pain at the source. Brain 140(10): 2570-2585.

Xie, X., C. Pascual, C. Lieu, S. Oh, J. Wang, B. Zou, J. Xie, Z. Li, J. Xie, D. C. Yeomans, M. X. Wu and X. S. Xie (2017). Analgesic Microneedle Patch for Neuropathic Pain Therapy. ACS Nano 11(1): 395-406.

Zhao, J. Y., L. Liang, X. Gu, Z. Li, S. Wu, L. Sun, F. E. Atianjoh, J. Feng, K. Mo, S. Jia, B. M. Lutz, A. Bekker, E. J. Nestler and Y. X. Tao (2017). DNA methyltransferase DNMT3a contributes to neuropathic pain by repressing Kcna2 in primary afferent neurons. Nat Commun 8: 14712.

Zhao, X., Z. Tang, H. Zhang, F. E. Atianjoh, J. Y. Zhao, L. Liang, W. Wang, X. Guan, S. C. Kao, V. Tiwari, Y. J. Gao, P. N. Hoffman, H. Cui, M. Li, X. Dong and Y. X. Tao (2013). A long noncoding RNA contributes to neuropathic pain by silencing Kcna2 in primary afferent

neurons. Nat Neurosci 16(8): 1024-1031.

JPET Fast Forward. Published on December 8, 2020 as DOI: 10.1124/jpet.120.000315
This article has not been copyedited and formatted. The final version may differ from this version.

Footnotes

a) All authors were employees of Haisco Pharmaceutical Group when the study was conducted.

b) Reprint requests should be addressed to

Jia Ni

Haisco Pharmaceutical Group Co., Ltd.

136 Baili Road, Wenjiang District, Chengdu 611130, China.

E-mail: nijia@haisco.com

JPET Fast Forward. Published on December 8, 2020 as DOI: 10.1124/jpet.120.000315
This article has not been copyedited and formatted. The final version may differ from this version.

Figure legends

Figure 1. Chemical structures (A) and *in vitro* potency (B) of HSK16149 and pregabalin. The *in vitro* potency was measured using [^{3}H]gabapentin binding assay in cerebral cortical membranes of male Wistar rats. Data are expressed as mean ± SD of duplicate determinations. Dotted lines indicate 95% CI.

Figure 2. Analgesic effects of HSK16149 and pregabalin in CCI model. (A – C) Time course for the effects of HSK16149 and pregabalin on neuropathic pain in rats. HSK16149 and pregabalin were orally administered and the mechanical thresholds were evaluated at different time points after dosing. The AUCs (50% PWT *vs.* time) were calculated with a trapezoid rule, and are shown in (D), (E) and (F). Data are expressed as mean ± SD (n=10/group). $^{*}P<0.05$, $^{**}P<0.01$, $^{***}P<0.001$ *vs.* vehicle, two-way ANOVA with Dunnett's multiple comparisons (A, B, C); $^{*}P<0.05$, $^{***}P<0.001$ *vs.* vehicle, Kruskal-Wallis test with Dunn's multiple comparisons (D, E); $^{*}P<0.05$ *vs.* vehicle, one-way ANOVA with Dunnett's multiple comparisons (F); $^{\#}P<0.05$, $^{\#\#}P<0.01$ *vs.* 10 mg/kg pregabalin, two-tailed, unpaired t-test (E); $^{\$}P<0.05$ *vs.* 30 mg/kg HSK16149, two-tailed, unpaired t-test (F).

Figure 3. Analgesic effects of HSK16149 and pregabalin in STZ-induced diabetic neuropathy. (A – C) Time course for the effects of HSK16149 and pregabalin on neuropathic pain in rats. HSK16149 and pregabalin were orally administered, and the mechanical thresholds were evaluated at different time points after dosing. The AUCs (50% PWT *vs.* time) were calculated with trapezoid rule, and are shown in (D), (E), and (F). Data are expressed as mean ± SD

JPET Fast Forward. Published on December 8, 2020 as DOI: 10.1124/jpet.120.000315
This article has not been copyedited and formatted. The final version may differ from this version.

(n=10/group). $^{*}P<0.05$, $^{**}P<0.01$, $^{***}P<0.001$ *vs.* vehicle, two-way ANOVA with Dunnett's multiple comparisons (A, B, C); $^{**}P<0.01$, $^{***}P<0.001$ *vs.* vehicle, Kruskal-Wallis test with Dunn's multiple comparisons (D, E, F); $^{\#}P<0.05$, $^{\#\#\#}P<0.001$ *vs.* 10 mg/kg pregabalin, two-tailed, unpaired t-test (E); $^{\$\$\$}P<0.001$ *vs.* 30 mg/kg HSK16149, $^{\&\&}P<0.01$ *vs.* 30 mg/kg pregabalin, two-tailed, unpaired t-test (F).

Figure 4. Antinociceptive effects of HSK16149 and pregabalin in ICS-induced fibromyalgia. HSK16149 and pregabalin were intragastrically administered at 2 h before the pain test was performed. Data are expressed as mean ± SD (n=10/group). $^{***}P<0.001$ *vs.* naïve, Kruskal-Wallis test with Dunn's multiple comparisons (A); $^{***}P<0.001$ *vs.* vehicle, $^{\#\#\#}P<0.001$ *vs.* naïve, Kruskal-Wallis test with Dunn's multiple comparisons (B).

Figure 5. Effects on pain behavior of HSK16149 and pregabalin in formalin-induced inflammatrory pain. HSK16149 and pregabalin were intragastrically administered at 2 h before formalin was injected. Data are expressed as mean ± SD (n=10/group). $^{***}P<0.001$ *vs.* vehicle, one-way ANOVA with Dunnett's multiple comparisons.

Figure 6. Ataxic (A) and sedative (B) side effects of HSK16149 and pregabalin. The tests were performed at 2 h post-administration. Data are expressed as mean ± SD (n=10/group). $^{*}P<0.05$, $^{**}P<0.01$, $^{***}P<0.001$ *vs.* vehicle, Kruskal-Wallis test with Dunn's multiple comparisons, $^{\#}P<0.05$ *vs.* 100 mg/kg HSK16149, two-tailed, unpaired Mann-Whitney U test (A); $^{***}P<0.001$ *vs.* vehicle, one-way ANOVA with Dunnett's multiple comparisons (B).

Table 1. Pharmacokinetic parameters of HSK16149 and pregabalin in two rat models of neuropathic pain

Compound	Dose (mg/kg)	PK parameter			
		CCI model		STZ model	
		C_{max} (μg/mL)	$AUC_{0\text{-}24h}$ (μg·h/mL)	C_{max} (μg/mL)	$AUC_{0\text{-}24h}$ (μg·h/mL)
HSK16149	1	0.69	1.46	0.62	1.55
	3	1.69	4.27	1.80	4.75
	10	6.13	15.41	4.51	18.94
	30	16.90	61.63	18.00	59.60
Pregabalin	1	1.43	5.55	1.67	6.45
	3	4.26	20.21	4.49	20.54
	10	12.83	58.42	13.73	63.36
	30	30.50	138.89	28.55	158.95

Table 2. Therapeutic index of HSK16149 and pregabalin

	Animal models	Compound		
		HSK16149	Pregabalin	Mirogabalin*
Pharmacological activities (MED, mg/kg)	CCI model	10	10	10
	STZ model	10	10	ND
CNS side effects (MED, mg/kg)	Rotarod test	100	30	10
	Locomotor activity test	100	100	25
Therapeutic index	Rotarod test	10	3	1
	Locomotor activity test	10	10	2.5

*The results were provided in supplemental data.

ND: not detected.

A

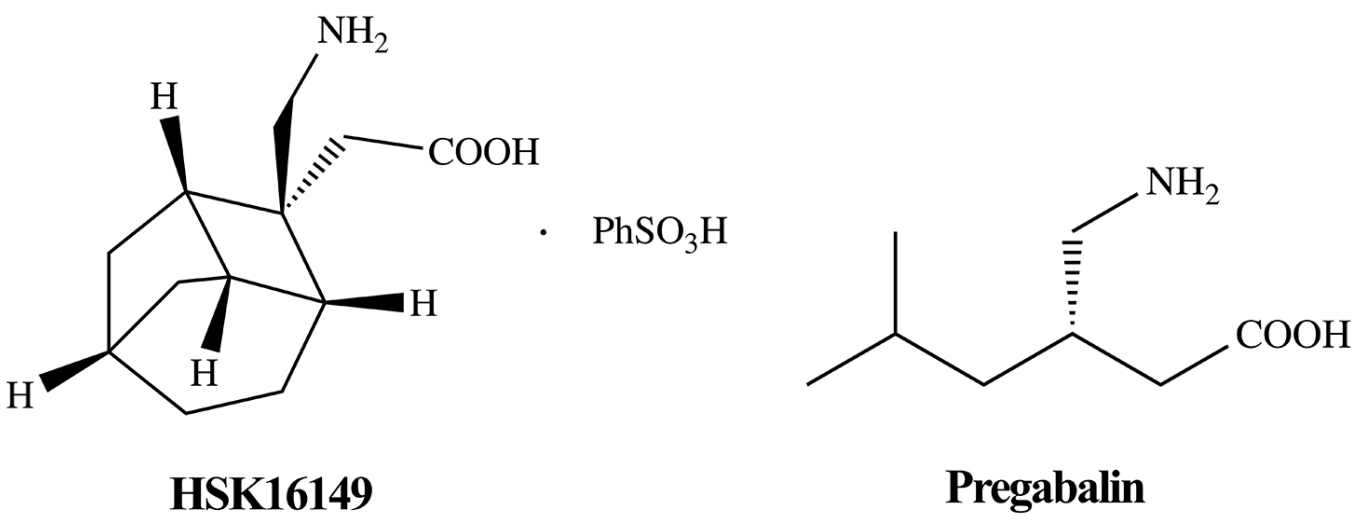

HSK16149 Pregabalin

B

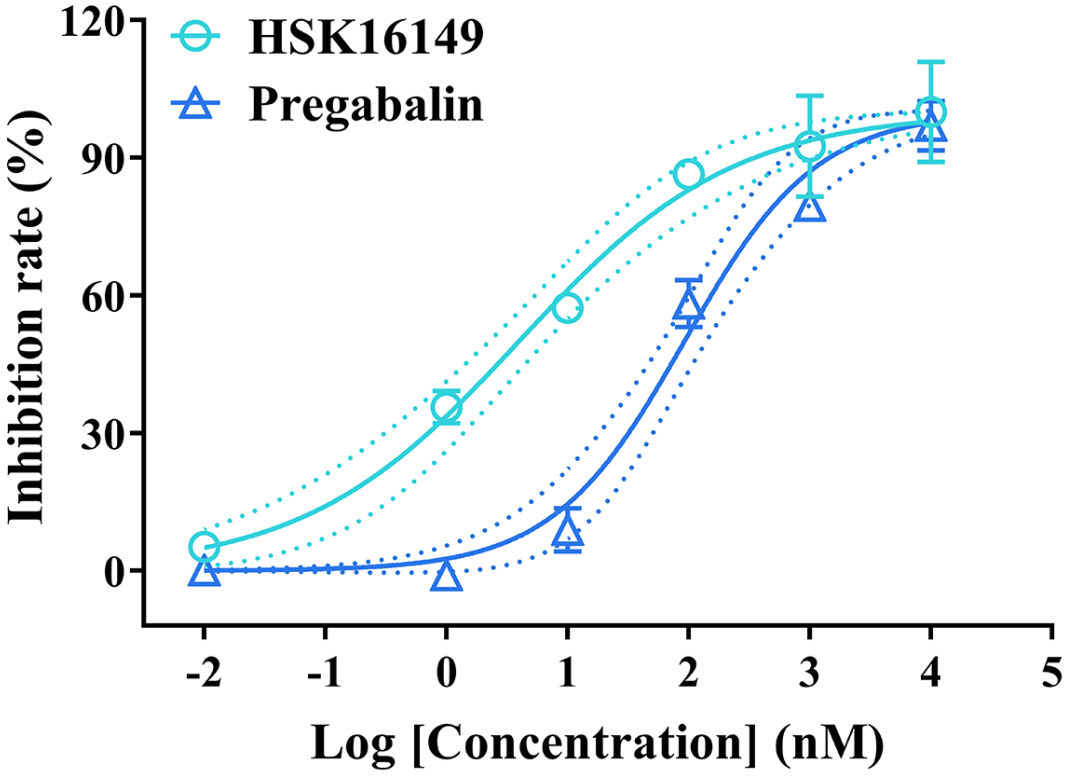

Figure 1

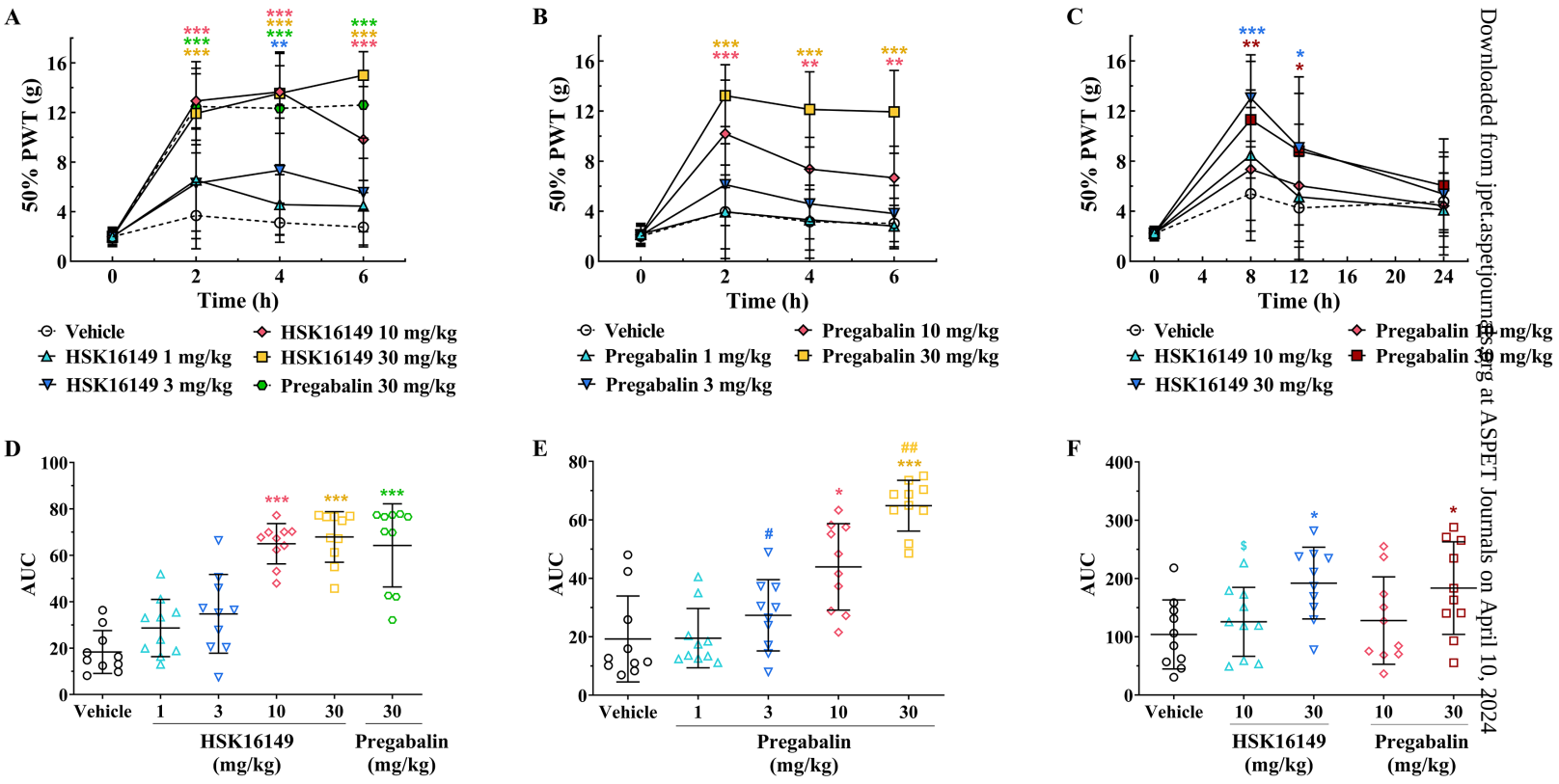

Figure 2

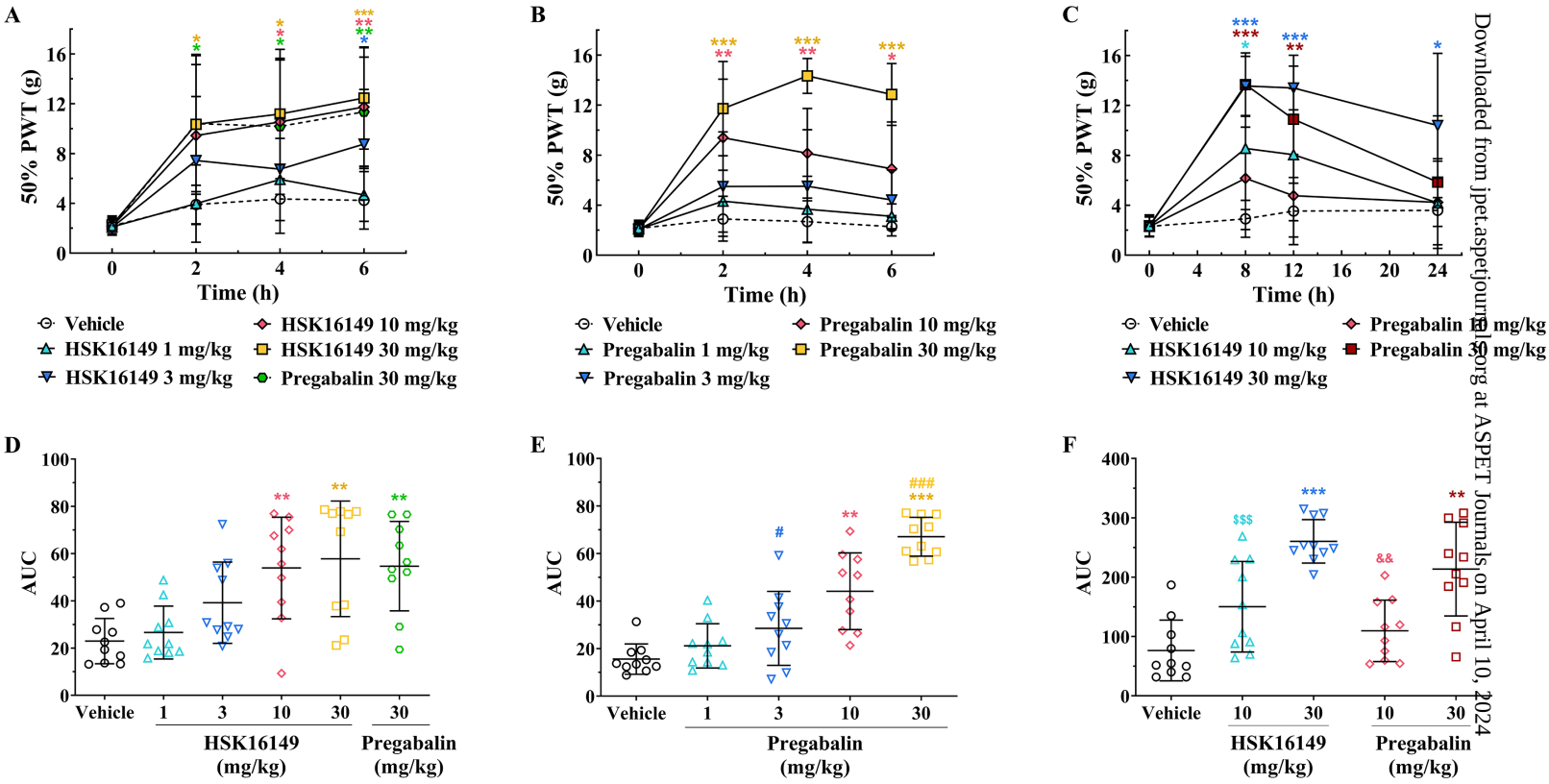

Figure 3

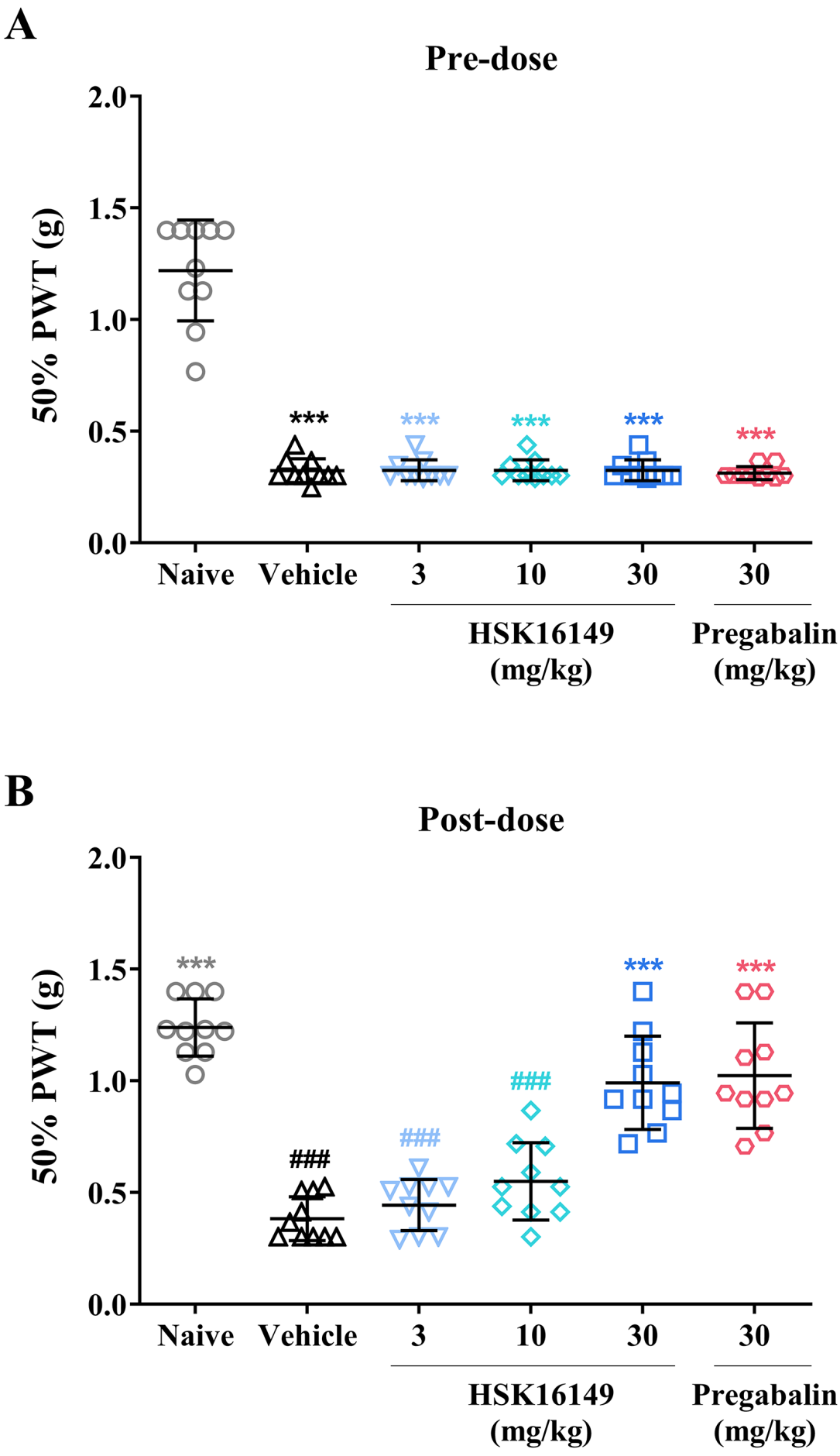

Figure 4

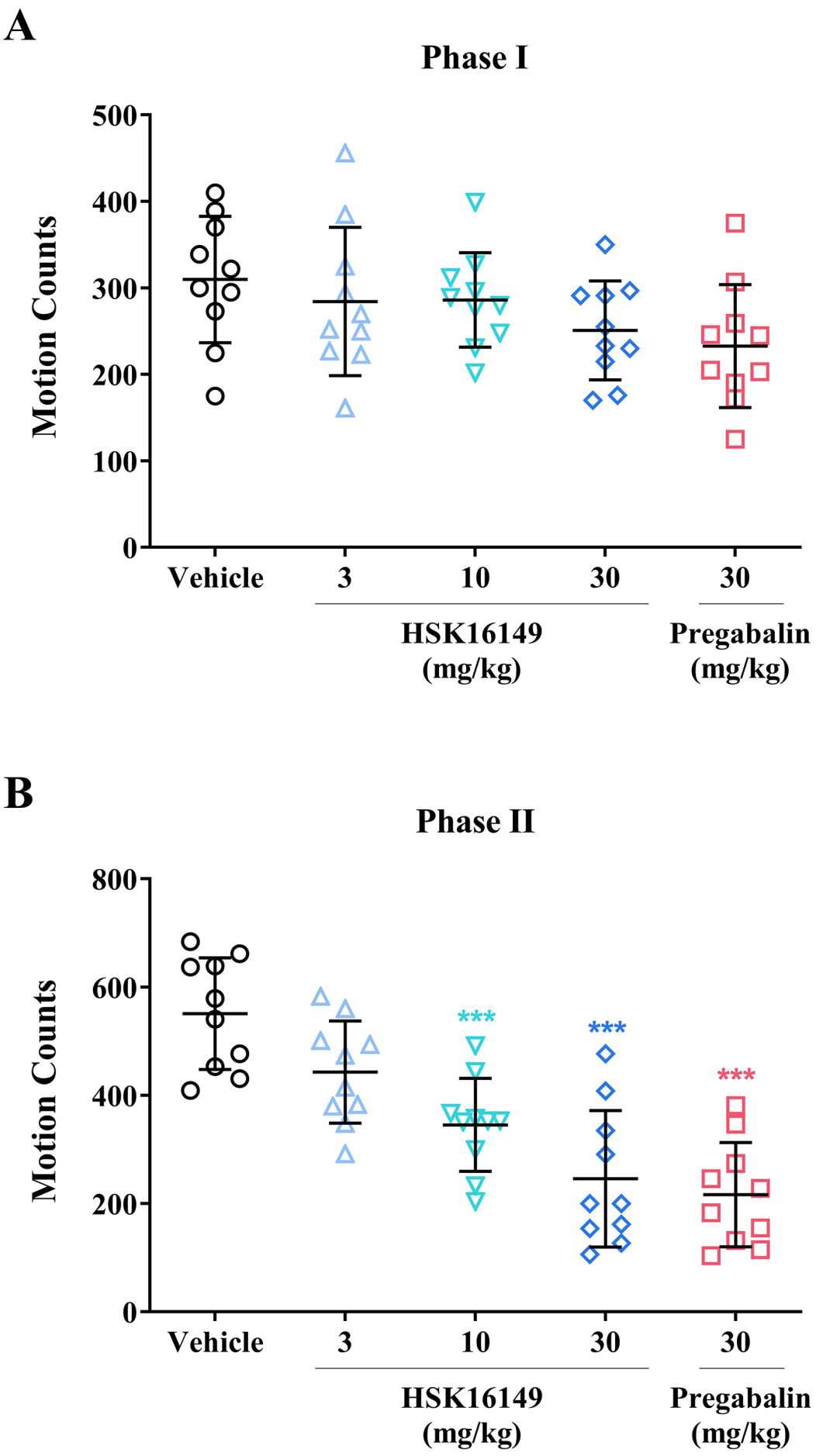

Figure 5

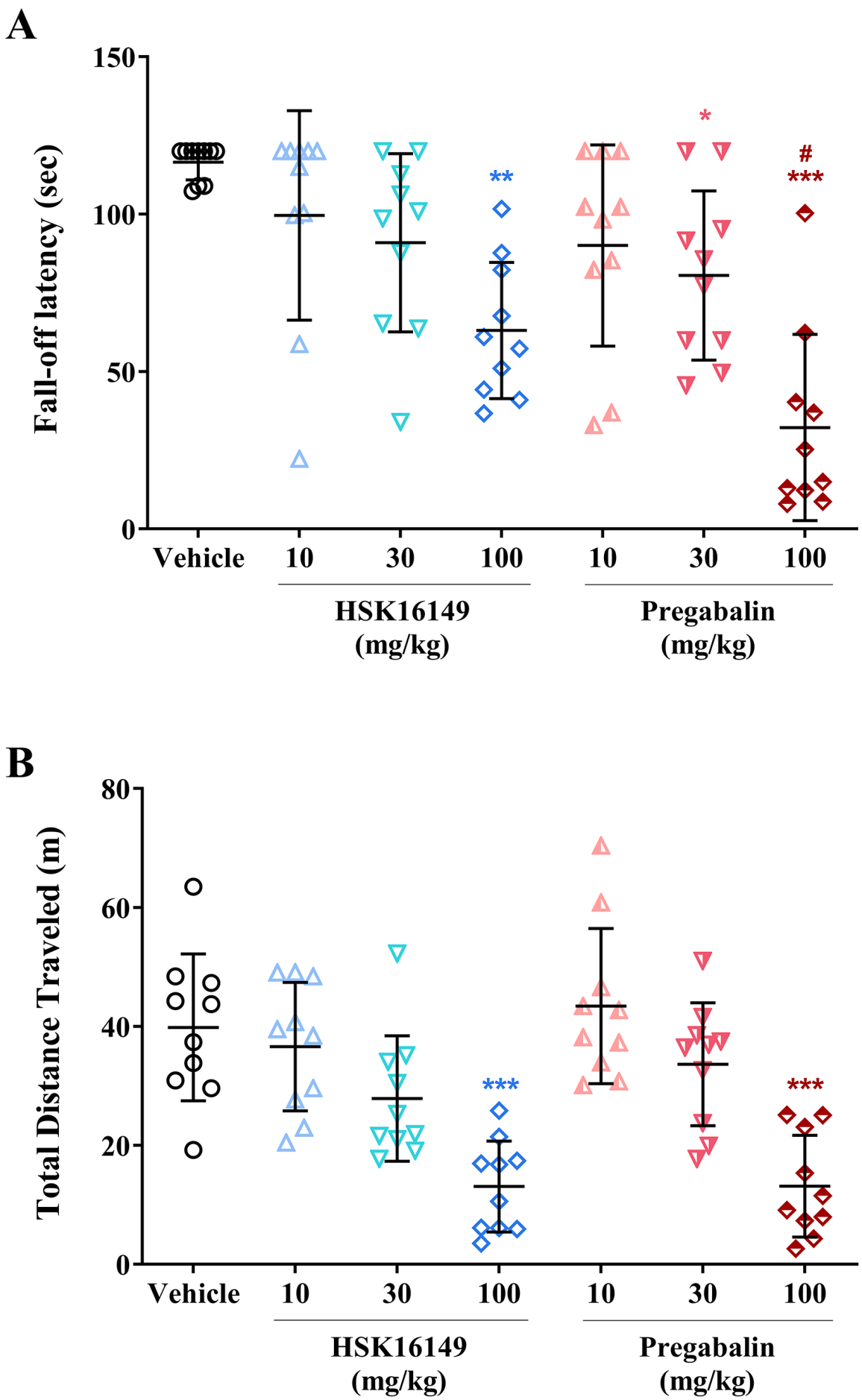

Figure 6

#JPET-AR-2020-000315R1

Supplemental data

Pharmacology and mechanism of action of HSK16149, a selective ligand of α2δ subunit of voltage-gated calcium channel with analgesic activity in animal models of chronic pain

Xiaoli Gou, Xiaojuan Yu, Dongdong Bai, Bowei Tan, Pingfeng Cao, Meilin Qian, Xiaoxiao Zheng, Lei Chen, Zongjun Shi, Yao Li, Fei Ye, Yong Liang* and Jia Ni*

Haisco Pharmaceutical Group Co., Ltd., 136 Baili Road, Wenjiang district, Chengdu 611130, China.

Supplemental materials and methods

Drugs and reagents

Mirogabalin was obtained from Medchem Express Co., Ltd. In all animal experiments, it was suspended in 0.5% methylcellulose and orally administered at a volume of 10 μL/g.

Tissue distribution studies

A total of 18 rats (N=3) were used to assess the tissue distribution of HSK16149 and pregabalin. Prior to the experiment, food was withheld overnight. The animals were orally administered HSK16149 or pregabalin at a dose of 30 mg/kg. Then, a blood sample (0.5 mL) was collected into a heparinized tube by puncturing the vena jugularis at 2, 4, or 6 h post-dosing, and the plasma sample was separated by centrifugation of the whole blood at 5000 ×*g* for 10 min at 4 °C. Subsequently, individual animal was euthanized, and the brain sample was removed, which was rinsed with cold saline and blotted dry with filter paper. Brain samples were homogenized in 50%

methanol (v/v) using Bertin Precellys Evolution. The concentrations of HSK16149 and pregabalin in plasma or brain tissue were detected using a validated liquid chromatography–tandem mass spectrometry method.

Supplemental Table 1. *In vitro* off-target pharmacological profile of HSK16149

Assay Name	Species	Conc. (μM)	Inhibition (%)/Agonist (%)
Adenosine A_1	human	10	-4
Adenosine A_{2A}	human	10	-2
Adenosine A_{2B}	human	10	-6
Adenosine A_3	human	10	3
Adrenergic α_{1A}	rat	10	3
Adrenergic α_{1B}	rat	10	-6
Adrenergic α_{1D}	human	10	0
Adrenergic α_{2A}	human	10	3
Adrenergic α_{2B}	human	10	6
Adrenergic β_1	human	10	-1
Adrenergic β_2	human	10	-3
Androgen (Testosterone)	human	10	14
Angiotensin AT_1	human	10	6
ATPase, Na^+/K^+, Heart, Pig	pig	10	-7
Bombesin BB1	human	10	15
Bradykinin B_1	human	10	5
Bradykinin B_2	human	10	-2
Calcium Channel L-Type, Benzothiazepine	rat	10	-14
Calcium Channel L-Type, Dihydropyridine	rat	10	-5
Calcium Channel L-Type, Phenylalkylamine	rat	10	1
Calcium Channel N-Type	rat	10	-7
Cannabinoid CB_1	human	10	-3
Cannabinoid CB_2	human	10	2
Chemokine CCR1	human	10	-4
Chemokine $CXCR_2$ ($IL\text{-}8R_B$)	human	10	-3
Cholecystokinin CCK_1 (CCK_A)	human	10	-11
Cholecystokinin CCK_2 (CCK_B)	human	10	-1
Cholinesterase, Acetyl, ACES	human	10	-6

Supplemental Table 1. *In vitro* off-target pharmacological profile of HSK16149 (continuing)

Assay Name	Species	Conc. (μM)	Inhibition (%)/Agonist (%)
Cyclooxygenase COX-1	human	10	22
Cyclooxygenase COX-2	human	10	4
Dopamine D_1	human	10	4
Dopamine D_{2L}	human	10	2
Dopamine D_{2S}	human	10	-2
Endothelin ET_A	human	10	1
Estrogen ERα	human	10	5
Fatty Acid Amide Hydrolase (FAAH)	human	10	-3
GABA (B1A/B2), Adenylyl Cyclase	human	10	5
$GABA_A$, Chloride Channel, TBOB	rat	10	-1
$GABA_A$, Flunitrazepam, Central	rat	10	-8
$GABA_A$, Ro-15-1788, Hippocampus	rat	10	1
$GABA_{B1A}$	human	10	1
$GABA_{B1B}$	human	10	-2
Galanin GAL1	human	10	-2
Glucocorticoid	human	10	5
Glutamate, AMPA	rat	10	-2
Glutamate, Kainate	rat	10	-6
Glutamate, Metabotropic, $mGlu_5$	human	10	-11
Glutamate, NMDA, Agonism	rat	10	1
Glutamate, NMDA, Glycine	rat	10	-1
Glutamate, NMDA, Phencyclidine	rat	10	10
Glutamate, NMDA, Polyamine	rat	10	-20
Glycine, Strychnine-Sensitive	rat	10	-1
Histamine H_1	human	10	3
Histamine H_2	human	10	0
Histamine H_3	human	10	-7
Interleukin IL-6	human	10	1

Supplemental Table 1. *In vitro* off-target pharmacological profile of HSK16149 (continuing)

Assay Name	Species	Conc. (μM)	Inhibition (%)/Agonist (%)
IP (PGI2)	human	10	20
Leukotriene, Cysteinyl $CysLT_1$	human	10	-8
Melanocortin MC_1	human	10	0
Melanocortin MC_4	human	10	-1
Monoamine Oxidase MAO-A	human	10	1
Monoamine Oxidase MAO-B	human	10	2
Muscarinic M_1	human	10	-3
Muscarinic M_2	human	10	2
Muscarinic M_3	human	10	-6
Muscarinic M_4	human	10	1
Neuropeptide Y Y_1	human	10	-8
Nicotinic Acetylcholine	human	10	-6
Nicotinic Acetylcholine α_1, Bungarotoxin	human	10	-11
Opiate δ_1 (OP1, DOP)	human	10	-5
Opiate κ (OP2, KOP)	human	10	2
Opiate μ (OP3, MOP)	human	10	-7
Peptidase, Angiotensin Converting Enzyme	rabbit	10	5
Peptidase, CTSG (Cathepsin G)	human	10	-3
Phosphodiesterase PDE3	human	10	-7
hosphodiesterase PDE4	human	10	-16
Platelet Activating Factor (PAF)	human	10	0
Potassium Channel [K_{ATP}]	hamster	10	10
Potassium Channel hERG	human	10	15
PPARγ	human	10	4
Progesterone PR-B	human	10	3
Protein Serine/Threonine Kinase, PKC, Non-Selective	rat	10	3
Protein Tyrosine Kinase, Insulin Receptor	human	10	0
Protein Tyrosine Kinase, LCK	human	10	2

Supplemental Table 1. *In vitro* off-target pharmacological profile of HSK16149 (continuing)

Assay Name	Species	Conc. (μM)	Inhibition (%)/Agonist (%)
Serotonin (5-Hydroxytryptamine) 5-HT_{1A}	human	10	1
Serotonin (5-Hydroxytryptamine) 5-HT_{1B}	human	10	11
Serotonin (5-Hydroxytryptamine) 5-HT_{2A}	human	10	3
Serotonin (5-Hydroxytryptamine) 5-HT_{2B}	human	10	13
Serotonin (5-Hydroxytryptamine) 5-HT_{2C}	human	10	-9
Serotonin (5-Hydroxytryptamine) 5-HT_3	human	10	11
Serotonin (5-Hydroxytryptamine) 5-HT_7	human	10	2
Sigma σ_1	human	10	9
Sigma σ_2	human	10	11
Sodium Channel, Site 2	rat	10	8
Tachykinin NK_1	human	10	6
Tachykinin NK_2	human	10	21
Tachykinin NK_3	human	10	-8
Transporter, Adenosine	guinea pig	10	-3
Transporter, Dopamine (DAT)	human	10	-4
Transporter, GABA	rat	10	7
Transporter, Norepinephrine (NET)	human	10	10
Transporter, Serotonin (5-Hydroxytryptamine) (SERT)	human	10	11
Uptake, Norepinephrine	human	10	8
Vasoactive Intestinal Peptide VIP_1	human	10	-1
Vasopressin V_{1A}	human	10	3

Supplemental Table 2. Pharmacokinetic parameters of HSK16149 and pregabalin in rat plasma and brain tissue.

Compound	PK parameter			
	Plama		brain	
	C_{max} (μg/mL)	$AUC_{0\text{-}6h}$ (μg·h/mL)	C_{max} (μg/g)	$AUC_{0\text{-}6h}$ (μg·h/g)
HSK16149	13.95	52.20	0.66	3.18
Pregabalin	80.57	307.13	12.65	57.18

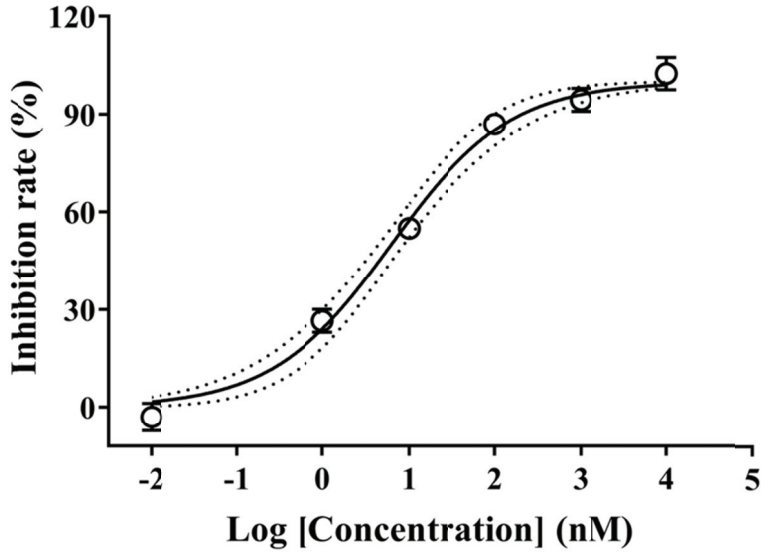

Supplemental Figure 1. The *in vitro* potency of mirogabalin. The study was conducted with a [^{3}H]gabapentin binding assay (Similar to Figure 1B). Data are expressed as mean ± SD of duplicate determinations. Dotted lines indicate 95% CI.

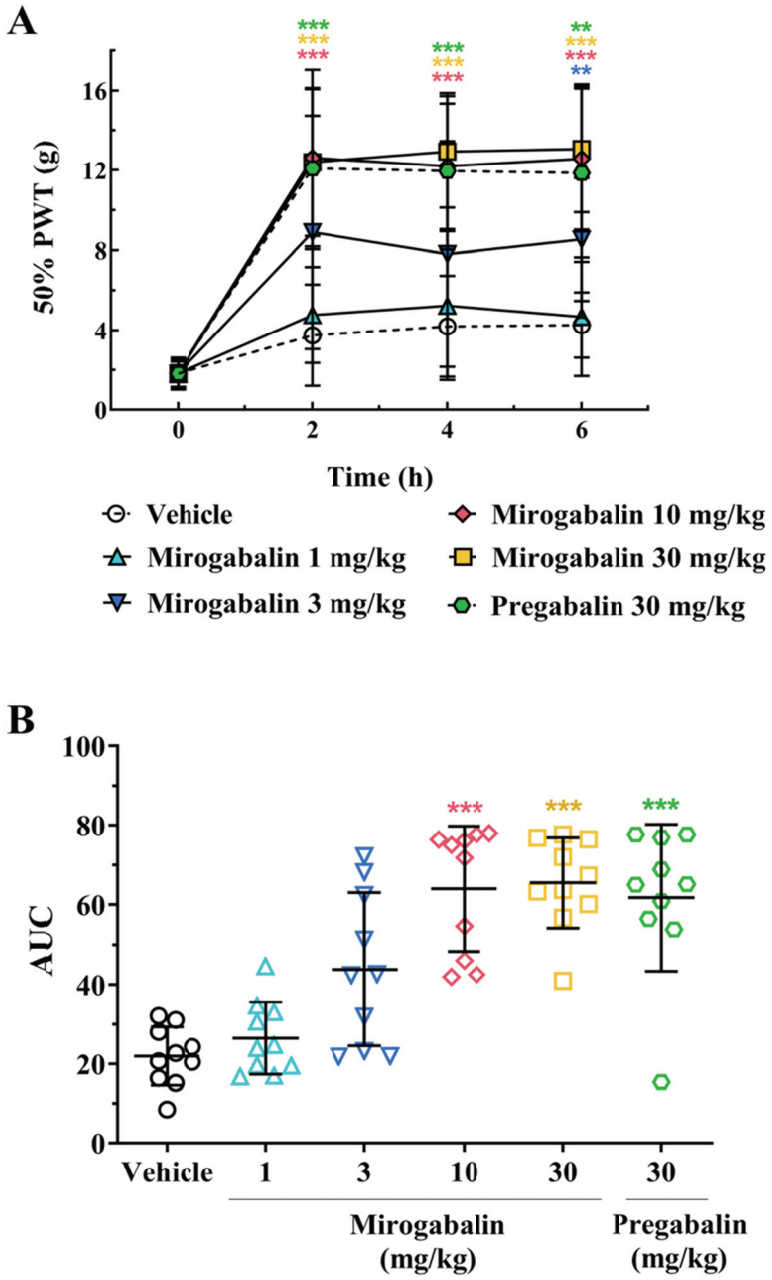

Supplemental Figure 2. Analgesic effects of mirogabalin in CCI model. On day 17 after the surgery was performed, mirogabalin were orally administered. The mechanical thresholds were evaluated at different time points after dosing. The AUC (50% PWT *vs.* time) was calculated with a trapezoid rule. Data are expressed as mean ± SD (n=10/group). $^{**}P<0.01$, $^{***}P<0.001$ *vs.* vehicle, two-way ANOVA with Dunnett's multiple comparisons (A); $^{***}P<0.001$ *vs.* vehicle, Kruskal-Wallis test with Dunn's multiple comparisons (B).

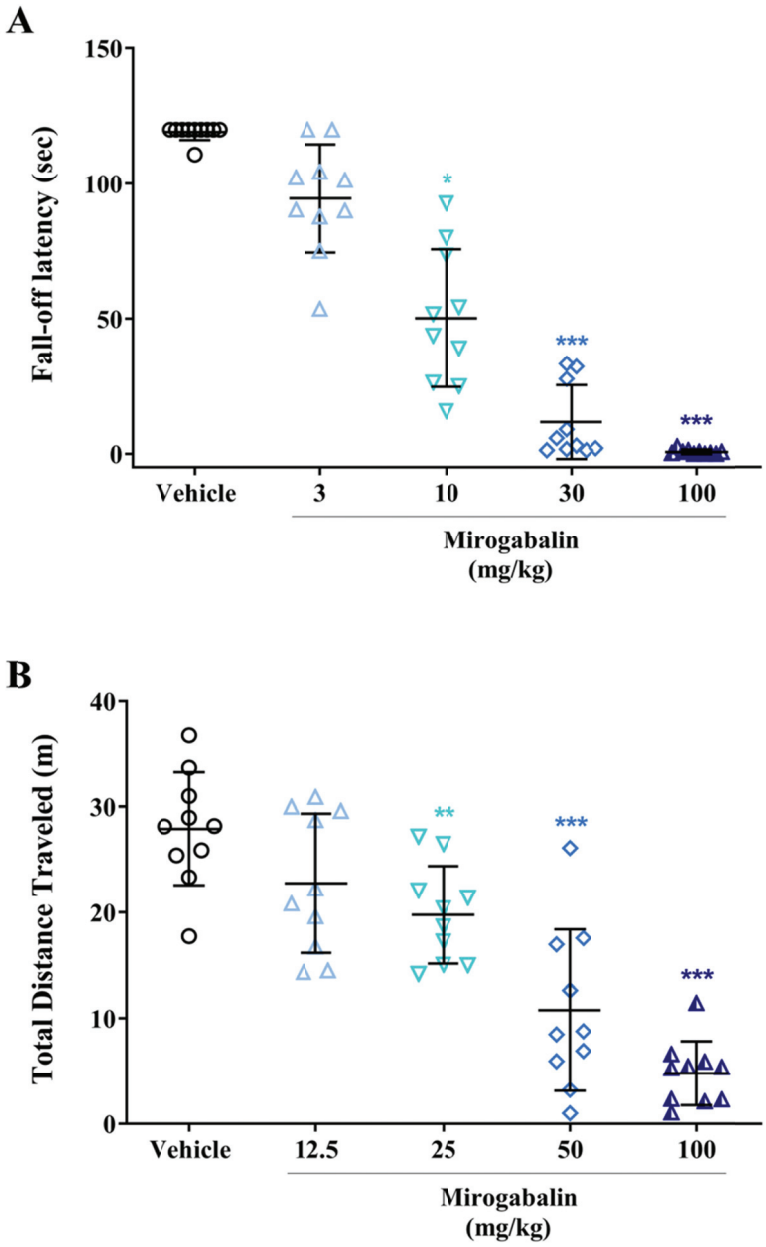

Supplemental Figure 3. Ataxic (A) and sedative (B) side effects of mirogabalin. The tests were performed at 2 h post-drug administration. Data are expressed as mean ± SD (n=10/group). $^{*}P<0.05$, $^{***}P<0.001$ *vs.* vehicle, Kruskal-Wallis test with Dunn's multiple comparisons (A); $^{**}P<0.01$, $^{***}P<0.001$ *vs.* vehicle, one-way ANOVA with Dunnett's multiple comparisons